Chapter 12

Remote Measurements of Ocean Currents Using Satellite-Borne Altimeters

Chapter Outline

Out of academic interest and for a variety of operational applications, it is often necessary to obtain a synoptic view of the spatial dimensions and patterns of water motion over several regions in the ocean under all weather conditions. Seawater motion mapping is useful in establishing large as well as comparatively small circulation routes and in detecting and identifying major ocean gyres. Direct measurement of large-scale ocean currents with current meter arrays is difficult and costly on basin scales. Unfortunately, oceanic water-motion features detected by visible and infrared imagery are sometimes contaminated by the influence of cloud, wind, and sea surface waves. Although passive microwave radiometry is free of cloud effects, higher sea states affect the emissivity. Another difficulty is a weak thermal signature in certain areas in some seasons.

The altimeter, on the other hand, senses oceanic water-motion features based on sea surface height variability and is, therefore, less affected by the mentioned meteorological effects. Furthermore, whereas sea surface images fundamentally provide a qualitative visual indication of the sea surface water-motion features from which water-motion velocity can be estimated using various algorithms, satellite altimetry directly provides quantitative information on various forms of seawater motion.

While we consider the altimetric method of oceanic current measurements, our interest is restricted primarily to boundary currents; variability of spatial length scales of less than 1,000 km, which is typical of most geostrophic circulation phenomena; and mesoscale phenomena such as gyres and rings (100−300 km range). In this case, the very long length-scale time variability in height caused by tides may interfere with the detection of these circulation features. This error can, however, be corrected by judicious use of tide models. Further, because tides have periodicities of approximately 12 hours, which is very much shorter than the lifetime of most circulation features, the effects of tides may be filtered out. Although the principle of sea-level measurement using altimeters may appear to be simple, much ancillary information as well as highly sophisticated mathematical algorithms are needed to arrive at error-free measurements. The altimetry data have begun to significantly improve our ability to understand oceanic water motion, which strongly influences weather and climate.

In satellite altimetry the sea level relative to a reference ellipsoid that best approximates the shape of the Earth is measured along the satellite ground track (see Wunsch and Gaposchkin, 1980). Because the reference ellipsoid best approximates the geometrical shape of the Earth, with the minor axis of the ellipsoid passing through the poles of the Earth and the major axis of the ellipsoid along the Earth's equatorial plane, the reference ellipsoid surface generally lies above the mean sea level (MSL) and below the mountain levels. For example, the ellipsoid height at the Lakshadweep Island region in the Arabian Sea in the Indian Ocean is ~92 m above the local MSL. In the context of examining satellite altimetric measurements for

Measuring Ocean Currents. http://dx.doi.org/10.1016/B978-0-12-415990-7.00012-0

oceanographic studies, a frequently used term is *marine geoid*. The marine geoid is a surface that would be assumed by the ocean surface if it were a motionless and uniformly dense fluid that is gravitationally bound to a rotating Earth. In other words, the geoid is an equipotential surface of the Earth's gravity field, to which a motionless ocean would conform. Often, the geoid lies far away from the Earth's reference ellipsoid, which is the smooth geometric surface approximating the shape of the entire Earth. Because of Earth's gravity variations, the shape of the geoid is often irregular and in some cases significantly departs from the reference ellipsoid. For example, across the narrow (200 km) Puerto Rico trench, the sea surface sharply dips downward 20 meters relative to the reference ellipsoid (Townsend, 1980; Cheney and Marsh, 1981). Likewise, there is a sharp rise in geoid over the Muir seamount north of Bermuda at about 33°N (Cheney et al., 1984).

The geoid surface is obtained quantitatively from models based on gravity measurements and long-term satellite data. For example, the model, called the PGS-S4, is based on the Goddard Earth Models but also contains Geos-3 and Seasat altimeter data (Cheney et al., 1984). The map of residual sea level (i.e., dynamic topography) is derived by subtracting the local geoid from the altimetric measurement (see Figure 12.1).

A major goal of satellite altimeter missions is the determination of the large-scale dynamic topography of the ocean. Important phenomena include the mean dynamic topography, changes in the mean height of the global ocean, and regional changes of dynamic topography on seasonal or interannual time scales. Knowledge of the mean structure of the dynamic topography is necessary for the determination of the general circulation of the ocean. Satellite altimeter measurements currently provide the only means for determining the level of the sea surface relative to the geoid on a global basis.

Interpretation of satellite altimeter measurements for oceanographic studies is limited by the errors in the marine geoid model. The ocean's surface, while appearing flat, is actually covered with a mosaic of hills, valleys, bumps, and dips caused by variations in Earth's gravity field, currents, winds, and tides. After subtraction of the contribution from Earth's gravity field (i.e., geoid), the residuals are usually smoothed so that only features of interest are retained. Wherever shipboard measurements of temperature and salinity, e.g., those by Levitus (1982), are available, the altimeter-derived dynamic heights can be cross-checked with those calculated from such *in situ* measurements. This will give us a better understanding of ocean circulation field and how it affects climate. The marine geoid was not well known locally before about 2004; therefore altimeters were usually flown in orbits that have an exactly repeating ground track.

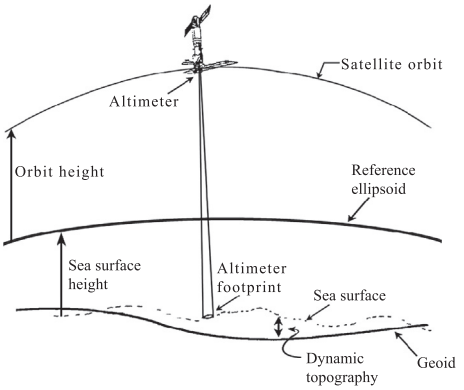

FIGURE 12.1 Concept diagram of satellite altimetry method of dynamic topography measurement.

Satellite altimeters profile the sea surface with extraordinary precision (a few centimeters) and provide new ways of studying ocean circulation. Altimetric maps of mean sea height have revealed the intricate surface expressions of meanders and eddies. Temporal variability of the sea surface due to meandering currents and eddies has been determined with an uncertainty of only a few centimeters, providing the first comprehensive view of the global eddy field. Even the broad, basin-scale circulation has been observed to a certain degree by subtracting the modeled gravimetric topography from global altimetric mean surfaces.

Superimposed on the static geoid topography is dynamic topography due to ocean circulation. Temporal variability of dynamic height due to oceanic eddies can be determined from time series of repeated altimeter profiles. Maps of sea-height variability and eddy kinetic energy derived from altimetry in some cases represent improvements over those derived from standard oceanographic observations. Measurement of absolute dynamic height imposes stringent requirements on geoid and orbit accuracies, although models and data have been used to derive surprisingly realistic global circulation solutions. Further improvement will be made only when advances are made in geoid modeling and precision orbit determination.

12.1. OCEANIC CURRENTS AND ASSOCIATED FEATURES GENERATED BY SEA SURFACE SLOPE

Geostrophic surface currents are maintained by horizontal pressure gradients and are expressed as sea-height slopes relative to the geoid. Although it is difficult to separate this dynamic component of sea height from the static geoid signal, an altimeter can readily detect the time-dependent variations in height. The most energetic fluctuations have typical scales of 100–300 km and are attributable to the ocean eddy field: meandering of narrow currents and migration of detached vortices. Eddying motions in the ocean are believed to be the dominant mechanism for transferring energy and momentum. Obtaining a basic description of the global distribution of mesoscale eddy

variability is fundamental to an improved understanding of ocean dynamics (Cheney et al., 1984).

Piling up or piling down of the sea surface relative to the neighboring water body results in characteristic slopes of the sea surface relative to the local marine geoid. Even in a homogeneous ocean, where density is constant, these slopes produce horizontal pressure gradients. The resulting seawater motion is generally called *slope current*. Because it is the pressure field that ultimately drives the slope current, in the literature these motions are also termed *near-surface geostrophic currents*. Because large-scale currents are very nearly in geostrophic balance, their velocity can be calculated from the pressure gradient on an equigeopotential surface. The surface geostrophic current therefore can be calculated from the deviation of sea level from the equigeopotential at the ocean surface (the marine geoid).

Because the primary contribution of altimetry is in the determination of sea surface-height variability, altimetric measurements can be employed to obtain a realistic view of ocean surface current. Measuring sea level from space by satellite altimetry thus offers a unique opportunity for determining the global surface geostrophic ocean circulation and its variability. Coupled with knowledge of the geoid and the ocean density field, satellite altimetry provides the only feasible approach for determining absolute geostrophic currents in the global ocean. Repeated altimetric observations of sea level at the same locations can resolve the variability of surface geostrophic currents, without the requirement for an accurate geoid model (Fu et al., 1988). The most energetic fluctuations of the slope current have typical scales of 100–300 km and are attributable to the ocean eddy field, meandering of narrow currents, and migration of detached vortices. Obtaining a basic description of global mesoscale eddy variability is fundamental to an improved understanding of ocean dynamics. The magnitude of dynamic sea surface elevation ranges from 10 cm (gyre-scale currents) to over 1 m (western boundary currents and eddies), with variance spread over a wide range of wave numbers and frequencies. The required measurement accuracy is thus dependent on the phenomenon of interest. Generally, an overall accuracy of better than 10 cm is required for observations of the dynamic sea surface elevation to be useful.

Temporal variability of the large-scale circulation is strongly linked to weather and climate. An example is the El Niño/Southern oscillation phenomenon in the Pacific. At approximately five-year intervals, patterns of atmospheric pressure and wind in the tropics undergo dramatic change. Easterly trade winds normally create westward currents along the equator and set up a zonal gradient of sea height as water accumulates in the west. During El Niño, trade winds may actually reverse, resulting in a redistribution of water back toward the east. During the 1982–83 event, sea-level changes of up to 40 cm were observed near the equator. Even as far north as 45°N along the North

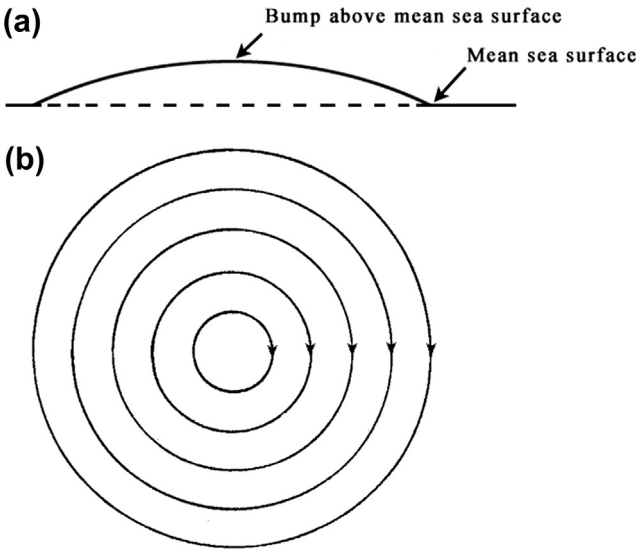

FIGURE 12.2 Concept diagram of a clockwise rotating warm-core circular eddy. (a) Vertical cross-sectional view of sea surface topography of the eddy; (b) plan view.

American coast, 35-cm monthly mean deviations were observed. These anomalous sea-level signals apparently propagate eastward across the central Pacific over a period of a few months. A satellite altimeter with a precision of a few centimeters can, in principle, provide a complete description of sea-level change on all scales.

In the open ocean, slopes of the sea surface can be generated if the wind distribution is not uniform. In such situations the water must pile up in the convergence zone, producing a slope of the sea surface in this zone. Boundaries of two distinct water masses (i.e., frontal region) also exhibit characteristic deviations from the mean sea surface, resulting in water-current motion along the front. Warm-core and cold-core eddies are also associated with characteristic sea surface slopes. For example, a warm-core eddy is associated with a "bump" of the sea surface at the core region (see Figure 12.2), whereas a cold-core eddy is characterized by a "dip" of the sea surface at the core region (see Figure 12.3).

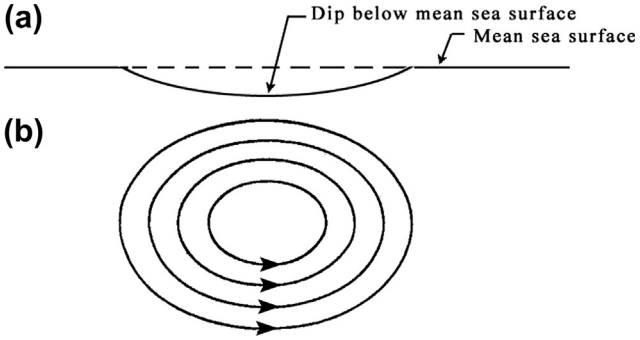

FIGURE 12.3 Concept diagram of a counter-clockwise rotating cold-core elliptical eddy. (a) Vertical cross-sectional view of sea surface topography of the eddy; (b) plan view.

The bumps and dips are caused by spatial variations in seawater density across the eddy region. In reality, several energetic oceanic regions are luxuriant in time-varying sea surface bumps and dips as a consequence of the temporal and seasonal evolution, growth, and decay of a variety of geostrophic currents and eddies. Such a fascinating model-simulated mosaic of mean sea surface heights (SSH) at contour intervals of 8 cm from the Atlantic Ocean, including the Intra-Americas Sea zoomed into the Gulf Stream region between Cape Hatteras and the Grand Banks (see Figure 12.4), has been reported by Hurlburt and Hogan (2008). The ocean eddy fields (typical scales of 100−300 km) have lifetimes ranging a few weeks to a few months. This topic was addressed in more detail in Chapter 1.

In coastal water bodies, interference by the coast to the slow westward drift of water mass results in its piling up on the western boundaries of the oceans. A current is generated to arrest continuous piling up. Because water mass piling up at the western boundaries of the oceans takes place continuously, as a counteracting mechanism the slope currents also persist without break. The slope currents generated along the western boundaries of the oceans are often termed *western boundary currents* (WBCs). The most prominent features in the Southern Hemisphere are the Agulhas Current off the tip of South Africa, the confluence of the Falkland and Brazil Currents east of Argentina, and the Antarctic Circumpolar Current, represented as a series of sea-level variability maxima surrounding Antarctica. Because of westward intensification of the wind-driven ocean currents, higher sea-level variability is most prevalent in the western parts of the oceans. Seamounts play an important role in controlling the water circulation in large ocean basins. For example, there is a marked contrast between the highly variable western North Pacific and the quieter eastern basin, with the dividing line occurring near the Emperor Seamount chain. This line of seamounts apparently acts as an efficient barrier to the high variability generated by the Kuroshio in the west.

Sea surface slopes have important implications in oceanography. For example, downward sea surface slope along the equator is responsible for the worldwide existence of a remarkably strong current, known as the *equatorial undercurrent*. This current, centered on the equator and flowing from west to east with a maximum speed of 100−150 cm/s, is ~200−300 km wide and ~150−300 m deep. It has been observed that the width, depth, and speed of this current can vary depending on the ocean and, probably, the season (Neumann, 1968). Similarly, the

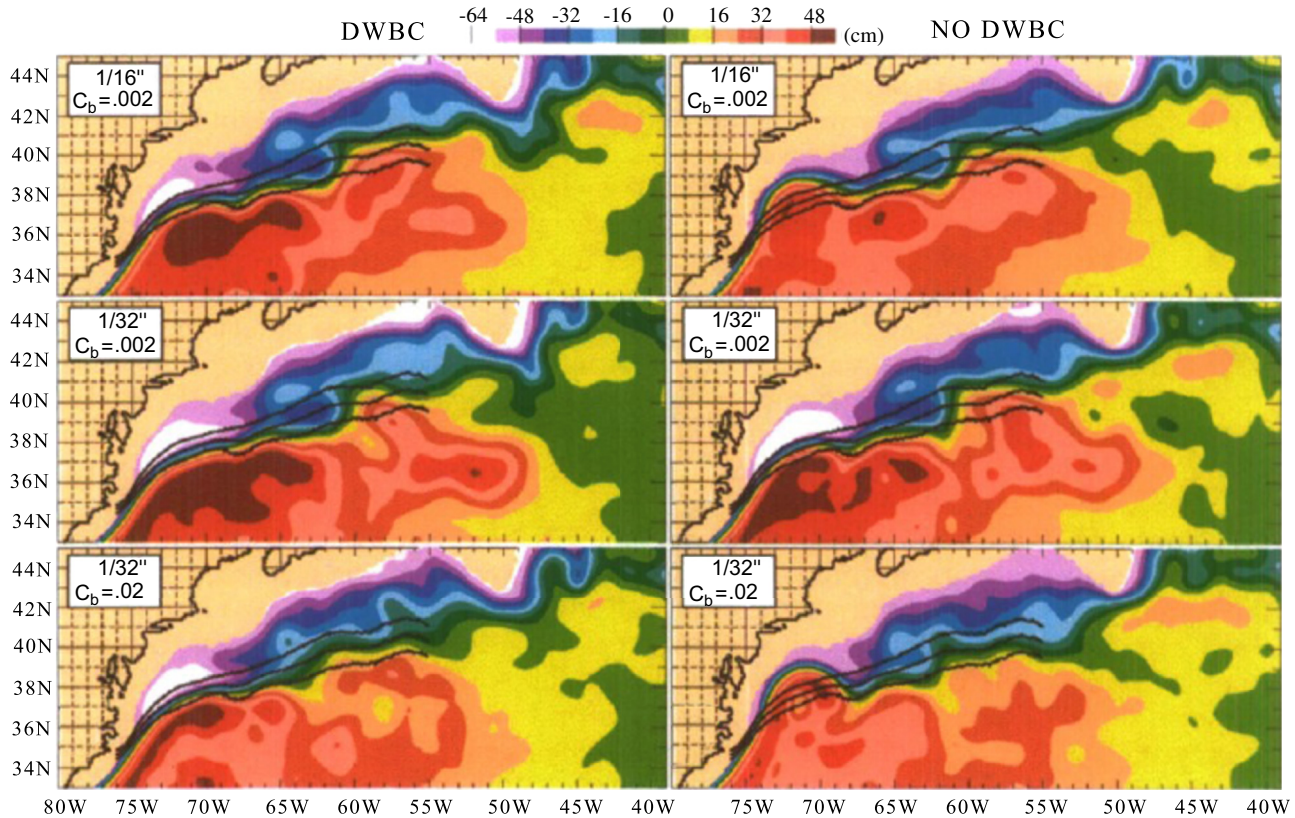

FIGURE 12.4 Model-simulated mosaic of mean sea surface heights (SSH) at contour intervals of 8 cm from the Atlantic Ocean, including the Intra-Americas Sea zoomed into the Gulf Stream region between Cape Hatteras and the Grand Banks, with and without Deep Western Boundary Current (DWBC). *(Source: Hurlburt and Hogan, 2008,* Dynamics of Atmospheres and Oceans*, Elsevier.)*

development of the Gulf Stream and the Kuroshio, which are two outstanding examples of WBCs, is associated with a westward displacement of the center of rotation of the subtropical gyres and the resulting piling up of water mass on the western boundaries of the respective oceans. In fact, detailed investigations have shown that the Gulf Stream is clearly detectable as a 100−200-cm step in dynamic height (Cheney et al., 1981).

12.2. DETERMINATION OF SEAWATER MOTION FROM SEA SURFACE SLOPE MEASUREMENTS

Slope currents, maintained by horizontal pressure gradients, are manifested as gradients of sea surface relative to an equipotential surface (i.e., the marine geoid). These currents can, therefore, be determined from precise measurements of sea surface slopes relative to the local marine geoid. The sea-level slope, tan β, is related to the associated slope current C by the relation (Neumann, 1968):

$$\tan\beta = (2\omega C \sin\varphi)/g \tag{12.1}$$

In this expression, β is the angle made by the instantaneous mean sea surface with the local marine geoid; ω is the angular velocity of Earth's rotation in radian/s (7.29×10^5 radian/s); φ is geographical latitude; and g is acceleration due to Earth's gravity. In this, (2ω sin φ) is popularly known as the *Coriolis parameter*, f. Thus,

$$C = (g \tan\beta)/f \tag{12.2}$$

If dz is the difference of the sea surface heights at two locations, separated by a horizontal distance dx, then the slope is given by $\tan\beta = dz/dx$, so that

$$C = (g/f)(dz/dx). \tag{12.3}$$

If the height of the sea surface relative to the marine geoid is ζ, then the u-component (u_s) and the v-component (v_s) of the surface geostrophic current can be related to surface elevation ζ by the expressions:

$$u_s = -\frac{g}{f}\frac{\partial\zeta}{\partial y}; \tag{12.4}$$

$$v_s = \frac{g}{f}\frac{\partial\zeta}{\partial x} \tag{12.5}$$

In practice, the residual height, ∂ζ, may be in cm or a few m, whereas the corresponding horizontal distance will be in hundreds of km. Because we can measure the surface topography from a satellite altimeter, we can calculate the slope of the sea surface and, in turn, the surface geostrophic currents. Typical slopes are ≈ 1−10 micro-radians for $v = 0.1$−1.0 m/s at mid-latitudes.

Sea surface slope across straits and channels can be determined using data from sea-level gauge records. This is possible because in coastal regions the absolute geodetic "zero" point can be established by precise leveling, and the mean sea level can be found from long-term sea-level observations. In fact, such observations, in conjunction with simultaneous current measurements in straits and channels, were used to test the validity of Equation 12.3. Using sea-level records from several islands and coastal stations in the equatorial Pacific Ocean, Wyrtki (1977) studied the response of the Pacific equatorial circulation to the 1972 El Niño. In fact, long-term sea-level records are considered an important source of data for the long-term monitoring of coastal currents and their variability.

Although it was known that currents generated by variations in sea surface slope due to actual piling up or removal of mass could be derived from precise sea surface leveling (Sverdrup et al., 1942), in the absence of necessary tools, slope-current measurements from the open oceans continued to remain a mere theoretical concept until satellite altimetry methods were introduced in the 1970s. If the satellite's instantaneous geographical position is independently determined, the sea surface dynamic topography can be inferred from the altimeter height measurements. With the availability of detailed geoid models, satellite altimetry has the potential for generation of near-synoptic maps of seawater motions and thereby to play a significant role in ocean circulation studies through its capability for rapid global observation of sea surface topography. Radar altimetry is identified as an important technology for the acquisition of data on oceanic large-scale water motions. In fact, the Gulf Stream path depicted by altimeter data agreed closely with analysis of simultaneously acquired satellite infrared imagery. Satellite altimetry can provide estimates of global surface geostrophic currents using surface height anomaly measurements (Fu and Chelton, 2001; Bonjean and Lagerloef, 2002). In fact, satellite altimetry has begun to demonstrate its capability to contribute significantly to the reliable mapping of geostrophic circulation of the oceans.

Apart from the well-known slope currents such as the WBCs and the Equatorial undercurrent, the other important oceanographic phenomena that influence the ocean surface topography include fronts, tides, swell waves, storm surges, and the more recently identified spatially fluctuating and circulating currents such as meanders and eddies, respectively. Determination of dynamic topography permits detection and quantification of these oceanic circulation features.

The most direct method of obtaining dynamic topography is to subtract a geoid model from the measured altimetric profiles. Although the detection of dynamic features from the altimeter profiles is straightforward in principle,

accurate determination of near-surface geostrophic circulation velocities (through the geostrophic relations 12.4 and 12.5) requires generation of a multitude of sea surface topographic maps using data from different passes of the altimeter in a given region of interest. The axis of water-motion trajectory can be estimated accurately from these multidirectional maps.

The launch of altimeter-borne polar-orbiting satellites was a major milestone in the remote measurement of sea surface parameters, including geostrophic circulation on an all-weather basis. The nadir (the region directly beneath the satellite) viewing radar altimeter measures the altitude of the satellite above the sea surface as follows:

The altimeter transmits a microwave signal of very short pulse width (a few nanoseconds) toward the terrestrial surface. The signal reflected off the sea surface is received back at the altimeter and the round-trip travel time (Δt) of the microwave pulse is measured. Assuming no significant radial motion of the satellite in the interval (Δt), the distance h between the altimeter's measurement point and the sea surface immediately below the altimeter is given by the relation:

$$h = C_m(\Delta t)/2 \tag{12.6}$$

where C_m is the speed of the electromagnetic wave in the medium that lies between the satellite and the sea surface bounded within the footprint of the altimeter beam. Subtraction of the detailed geoid (along the trajectory of the altimeter footprints) from the altimeter-measured height profiles at close spatial intervals along the satellite ground track yields profiles of residual sea heights (i.e., topographic maps) along that track. The residual sea-height variability, in part, represents the geostrophic height variability that generated the slope currents. Because the Earth spins toward the east, the satellite orbit has a westward drift relative to the Earth's surface. This drift facilitates generation of topographic maps along adjacent tracks and thereby ensures that the satellite altimeter provides a global coverage every few days.

Such maps at close grids contain data on sea surface slopes relative to the local marine geoid, which, in turn, contain information on ocean circulation dynamics. Combined with detailed marine geoid models, the altimeter data can therefore provide descriptions of the near-surface geostrophic current field. This information, together with subsurface measurements of the density structure, may also permit estimation of the velocity field at all depths (Marsh et al., 1982). While addressing the satellite altimetry method of ocean circulation measurements (schematically shown in Figure 12.1), it would be worthwhile to realize that the sea surface is characterized by oscillations and fluctuations associated with long-wavelength ocean tides, short-wavelength gravity waves and ripples, wind set-up/set-down, and inverse barometric effects. Tides in the open ocean are of comparatively small amplitudes (less than a meter). However, waves and inverse barometric effects can have large amplitudes (one to several meters). Fortunately, because the footprint of the altimeter on the sea surface runs to a few square kilometers, errors resulting from the presence of short-wavelength phenomena such as waves and ripples are smoothed out spatially. In effect, the altimeter measures, therefore, the distance to the "instantaneous mean" sea level.

12.3. TECHNOLOGICAL INTRICACIES IN REALIZING SATELLITE ALTIMETRIC MEASUREMENTS

Altitude measurement using a radar altimeter is simple in principle. However, considering the large distance between the satellite and the sea surface (~800−1,300 km), attaining a precision better than 10 cm (required for circulation studies) is a difficult task. Better precision in altitude measurement demands that the transmitted pulse be of extremely narrow width and that the pulse travel time be measured with utmost precision. Because the frequency bandwidth necessary for a pulse is the reciprocal of the pulse width, a sharper transmission pulse necessitates a wider frequency band to carry it. Even if a narrow pulse can be transmitted, with all the attendant constraints, a wave-laden sea surface causes the returned signal to be stretched out. The short pulse of the altimeter is "stretched" by the waves because scattering occurs from crests through troughs as the spherical pulse progresses downward (Barrick et al., 1980). Such degradation of the radar pulse shape leads to errors and adversely affects the altimeter's range resolution. Errors can creep into the calculation of the altitude also because of the variability of the speed (c) of the electromagnetic signal in the ionosphere and in the troposphere. Corrections must be applied to reduce all these errors.

Reduction in radar transmission pulse width to achieve better range resolution prevents injecting sufficient power into the transmission signal. On the other hand, sufficient power has to be injected into the narrow transmission pulse so that the returned signal is sufficiently stronger compared to the ambient noise. The return signal level is proportional to the amount of energy transmitted. The S/N power ratio at the input of the satellite-borne receiving system can be made considerably larger than unity by transmitting very high power. Unfortunately, it is often inconvenient to generate a very high peak power when the source is electronically driven, because the peak power is limited by the amplifier. These conflicting requirements of a high-resolution pulse radar altimetry are met by ingenious techniques such as pulse compression and pulse-limited modes of operation.

In the pulse compression process, a narrow pulse is dispersed by a filter into a very much longer "chirp" waveform (linearly varying frequency; see Figure 12.5a) in the transmission section, and the signal received from the sea

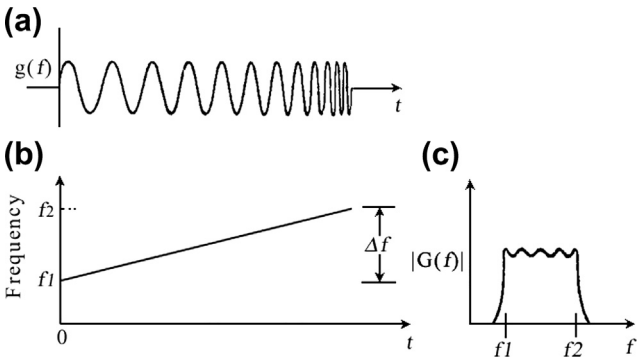

FIGURE 12.5 Representation of (a) chirp signal pulse, (b) frequency of chirp signal as a function of time, and (c) power spectrum of chirp signal pulse. *(Source: Clay and Medwin, 1977.)*

surface is compressed in the receiver section. Mathematical treatment of chirp pulse may be found in Biggs and Jordan (1989). As discussed here, the longer chirp signal permits transmission, with a lower peak power of an equivalent energy in a high-amplitude, narrow sine-wave pulse and achieving comparable fine-range resolution of a narrow sine-wave pulse. By linearly varying the frequency of the signal during transmission, it becomes possible to send a long pulse, keeping the bandwidth large. The transmission starts at frequency f_1 and then sweeps to f_2. The frequency bandwidth of this signal is $(f_2 - f_1) = B$. The superb capability of the long chirp signal to achieve fine-range resolution arises from the wider bandwidth associated with the frequency modulation to this pulse (Ulaby et al., 1982). Because the bandwidth, B, of the chirp signal is considerably larger than the reciprocal of its width τ, better temporal resolution and therefore better range resolution are achievable from a chirp signal relative to that from a sine-wave pulse of the same width τ. It may be recalled that the bandwidth of a sine-wave pulse of width τ is equal to $(1/\tau)$.

Often, a dispersive delay line (DDL) generates the basic linear FM (chirp) pulse. The heart of the DDL is a surface acoustic wave (SAW) device fabricated on a lithium tantalate substrate. In operation, an impulse of the desired high frequency is applied to the SAW filter, which then generates an expanded chirp pulse with the characteristic of linearly varying frequency. The frequency of the chirp signal as a function of time is shown in Figure 12.5b. The power spectrum of this chirp signal is shown in Figure 12.5c. The turn-on and turn-off transients broaden the spectrum outside f_1 and f_2. The total pulse duration is τ, and its frequency bandwidth after modulation is B. In the transmit mode, the chirp pulse is amplified to the required power level. In the receive mode, the dispersed pulse reflected from the terrestrial surface is compressed in a way that the signal at the output of the receiver system is sufficiently strong. This "de-chirping" process is accomplished by passing the received signal through a delay line-cum-adder system of which the time delay is a function of frequency. The time delay is such that the frequency element of the chirp signal first received from the terrestrial surface is delayed long enough so that it arrives at the output of the receiver system at the same time as the frequency element received last. All the frequencies in between also arrive at this time so that they are superimposed at a single instant of time in the receiver output. This is shown in Figure 12.6.

A particular combination of time delays matches the waveform of a particular signal. This combination is called a *matched filter*. If the filter is truly a matched filter, the time delays suffered by each point of the received chirp signal

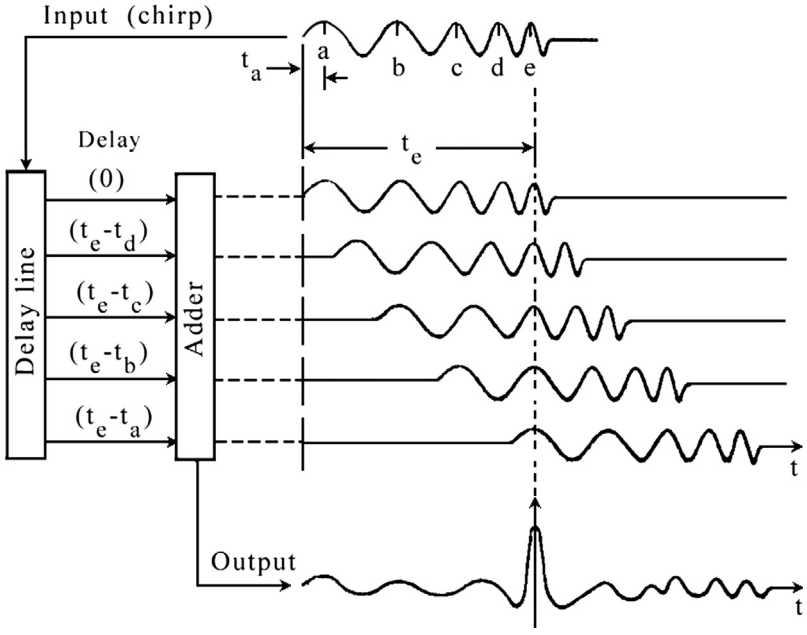

FIGURE 12.6 Schematic diagram illustrating the generation of a narrow peak signal from a long chirp signal when the chirp signal is delayed and added. *(Source: Clay and Medwin, 1977.)*

within the delay line will be such that addition of the various time-delayed signals would generate a very narrow peak with a fixed time delay relative to a fixed temporal position of the received signal. If a different signal, such as a down-swept chirp, is passed through an up-swept chirp matched filter, the output will be low-amplitude wiggles and no peak (Clay and Medwin, 1977). Referring to Figure 12.6, addition of signals with delay times $(t_e - t_d)$, $(t_e - t_c)$, $(t_e - t_b)$, and $(t_e - t_a)$ aligns the peaks of all the delayed signals in the receiver section in such a way that the desired narrow pulse is generated. The matched filter thus compresses the long transmission chirp pulse into a narrow peak. The low-amplitude wiggles, before and after the narrow peak, are called the *side lobes* of the matched filter. If B is the bandwidth of the transmitted chirp pulse, the effective width of the de-chirped signal at the receiver filter output is $(1/B)$. If the amplitude of the reflected linear FM chirp pulse is constant, the de-chirped signal takes the form of a $((\sin x)/x)$ pulse. The amplitude of the de-chirped signal is increased from 1 for the signal at the filter input to $\sqrt{(B\tau)}$ for the de-chirped waveform. The de-chirping is, therefore, an efficient way of achieving a narrow signal of higher amplitude for a given bandwidth of the transmission chirp signal. An excellent mathematical treatment of the chirp signal and a matched-filter implementation technique for a linear-FM chirp signal may be found in Ulaby et al. (1982).

Returning to the individual measurement of altitude to be representative of a small area, it is necessary that the altimeter footprint on the sea surface be of a minimal size. When one considers the large altitude of the satellite above the terrestrial surface, generation of a radar beam that is sufficiently narrow so that it is sharply focused onto a small area on the sea surface would require far too large an antenna aperture to be practical. Because operation in this ideal situation (i.e., beam-limited geometry) is difficult to achieve, an innovative technique known as *pulse-limited geometry,* which effectively achieves the function of beam-limited geometry, began to be used in precision altimeters. The pulse-limited geometry permits pulse transmission in a wide beam. This technique also minimizes the effects of antenna pointing errors, induced by variations in the attitude of the spacecraft, on height measurement precision (MacArthur, 1976). In this technique, a pulse is transmitted from a satellite and is radiated in a spherical shell, of which the intersection with the ocean surface defines an instantaneous illuminated area.

The leading edge of the transmitted pulse strikes the sea surface first immediately beneath the satellite and then moves out in a circular front. The trailing edge does the same a little later, resulting in the illuminated area being first a circle of growing area, from zero to a maximum when the rear of the pulse just touches the sea surface and then an annulus of constant area. Because the energy reflected from the sea surface is proportional to the illuminated area, the average return energy exhibits a linear initial rise and is followed by a plateau region resulting from the constant area of the expanding (but thinning) annulus. Each individual return is similar to the noise that results from the interference between reflections from multiple facets. Ultimately, the overall antenna pattern causes the signal return to attenuate. Geometries of pulse-width-limited mode of operation are given by MacArthur (1976) and Raney (1998). Altitude measurement is implemented based on leading-edge tracking of the pulse-width-limited sea surface return signal. The timing algorithm fits a curve to the leading edge of the return signal up to its maximum. This scheme ensures that the effective area of which the height is sampled is the illuminated circle just before it becomes an annulus. For a calm sea and a pulse length of t_p, this illuminated circle has a radius given by (Robinson, 1985):

$$R_a = \sqrt{(2hct_p)} \tag{12.7}$$

In this expression, h is the height of the satellite above the mean sea level and c is the speed of electromagnetic signal in the medium of travel. The area, given by $\pi(r_a)^2$, is substantially smaller than the best beam-width-limited footprint achievable by the present technology. For example, for Seasat with h and t_p 800 km and 3 nanoseconds, respectively, the value of r_a works out to be 1.2 km. With a beam as narrow as 1.59° at −3 dB, the beam-width-limited circular footprint associated with the Seasat-A altimeter radar had a radius of 11.1 km (Townsend, 1980). It can be seen that the area of the effective pulse-width-limited footprint (4.52 km^2) for a smooth surface is substantially smaller than that of an appreciably good beam-width-limited footprint (386.88 km^2). For a rough sea with "significant wave height" H, the radius of the illuminated circle just before it becomes an annulus is given by:

$$R_a = \sqrt{(2hct'_p)} \tag{12.8}$$

In this expression, $(t'_p)^2 = (t_p)^2 + (16\,H^2 \ln 2)/c^2$. For very calm seas, the leading edge is sharply defined. For rough seas, where the crest-to-trough distances are substantially greater than the altimeter's basic resolution, the leading edge of the incoming signal echo is stretched out in time, and the point on the leading edge corresponding to the mean sea level is not clearly defined. Thus, the sea state-related alteration of the characteristic shape of the sea surface return signal introduces an error in the determination of a spot value of altitude. These errors are, however, reduced by advanced signal tracking, modeling, and averaging techniques such as those described by MacArthur (1976) and Townsend (1980). The average of many samples acts to reduce the statistical fluctuations inherent in the individual waveform samples and minimizes noise.

12.4. CORRECTION OF ERRORS IN SATELLITE ALTIMETER DATA

Although the satellite altimetry method of near-surface oceanic current measurements might seem simple in principle, the actual implementation involves numerous technical hurdles that need to be taken care of before reliable measurements can be achieved. The measured height of the satellite above the sea surface at any instant in time must be corrected for a myriad of instrumental and geophysical effects. These include:

- Satellite height errors resulting from atmospheric-related effects in the electromagnetic pulse travel time
- Sea-state related errors
- Random errors resulting from long wavelength uncertainty in the orbital radius
- Errors arising from the unknown marine geoid

These aspects are briefly addressed in the following sections.

12.4.1. Correction of Satellite Orbit Errors

The orbit of the satellite (800 to 1,300 km above Earth's surface) does not remain precisely stable due to many atmospheric, astronomical, and geophysical forces that act to disturb the dynamics of the satellite. Other small orbit distortions are introduced by changes of the satellite's mass after maneuvers, by gravitational attractions of the moon and the sun, and even by the changes of gravity due to the water mass movements of the ocean tides. Apart from these uncertainties, because the microwave pulse transmitted from the satellite travels through the atmosphere, its round-trip travel time (Δt) must be corrected for propagation delays to accurately obtain the radial height (h) of the altimeter above the sea surface. The atmospherically induced delay in the radar pulse travel time is one of the primary corrections that must be applied to the radar altimeter measurements. The atmospheric effect can be separated into tropospheric and ionospheric effects. The tropospheric effects result in a decrease in the local speed of the electromagnetic signal due to the refractive index changes of the medium of propagation, caused by water vapor and other gases in the troposphere. Similar effects result from the presence of free electrons in the ionosphere. Tapley et al. (1982) discussed the errors due to these effects. It has been noticed that errors in sea-level estimates and water vapor content in the atmosphere are strongly correlated. The amplitude of the water vapor correction to the altimeter path length ranges from approximately 35 cm in the tropics to near zero at the poles and can be modeled with an uncertainty of ~5 cm for monthly means (Cheney et al., 1991).

Most of the atmosphere-related errors are corrected using data collected by other sensors on board the satellite (e.g., wet tropospheric correction to the measured altitude achieved using data collected by the satellite-borne scanning multichannel microwave radiometer [SMMR]). The SMMR measures the integrated mass density of the atmospheric water vapor along a line of sight from the SMMR antenna to the sea surface, thereby obtaining a measure of the increase in the effective radio-frequency path length (Tapley et al., 1982). In a satellite-based system, another source of water vapor data is the Special Sensor Microwave Imager (SSMI). The SSMI data enable derivation of global water vapor fields that provides an altimeter height accuracy of ~2 cm. In fact, for certain oceanographic applications, there is no substitute for a radiometer on board the altimeter satellite.

Errors resulting from ionospheric delay of the microwave signal can be corrected by the use of a dual-frequency altimeter (Lorell et al., 1982). This is possible because, for a given value of the columnar electron content along a ray path, the delay is inversely proportional to the square of the frequency.

Another atmospheric-related error, arising from rain and cloud effects, is caused by the spatial inhomogeneity of the medium of travel of the electromagnetic pulse. This inhomogeneity causes energy in different parts of the altimeter footprint to be attenuated differently, resulting in a distorted return waveform signature. This effect, in turn, causes mean-sea-level errors when standard tracking algorithms, which are dependent on pulse shape, are employed. To avoid misleading interpretation, the use of some kind of a sensor to detect the presence of rain is recommended so that such data can be flagged as questionable.

Separation of the variability in sea surface height, relative to the marine geoid, from the altimeter-measured height requires an independent determination of the radial component of the satellite orbit relative to a common-center-of-mass coordinate system. A dominant contributor to the random errors that creep into a satellite altimeter system is the long-wavelength uncertainty in the orbital radius. Another error is the deviation of the satellite track from the expected ground track. One of the reasons for changes in the satellite orbit is the atmospheric drag. One method of reducing this error component is to increase the altitude of the orbit. At higher altitudes, the atmospheric drag is comparatively lower. Above 1,300 km, the atmospheric drag is small enough that orbital errors may almost be neglected.

Another possibility to reduce satellite orbital error is to carefully design the satellite so as to minimize the effects of surface forces such as drag and solar radiation pressure. These methods can be implemented in a satellite, which is dedicated to altimetry alone. However, in a satellite where various sensors with conflicting altitude requirements are to be installed, these methods of orbit error minimization are difficult to be fully incorporated. Consequently, some sort of a compromise will have to be reached. One method of measuring the orbital radius error is frequent altimeter calibrations. A rather simple method is the use of sea-level gauge data. It has been shown by Wunsch (1986) that

calibration by a comparatively modest network of sea-level gauge systems can considerably reduce the overall error in the global estimates of large-scale oceanic water motions.

Because of these several uncertainties, the satellite positions and velocities must be tracked at intervals relative to fixed ground stations. An effective method of satellite altimeter calibration is by comparison with laser altimeter measurements as the satellite passes directly over ground-based laser-tracking stations, which are installed at selected locations (Joseph, 2000). During the calibration process, suitable corrections are applied to the laser-tracking station elevation based on the known local marine geoid and a myriad of optical and microwave propagation path-length effects. The calibration is repeated for many satellite passes over the laser-tracking stations. The microwave propagation effects are corrected using meteorological data acquired around the time of each pass. Because no ground-tracking stations are installed in the open ocean, the orbit of the satellite in these areas must be estimated using the calibration data as one of the inputs.

Laser- or microwave-tracking systems, which measure the range or Doppler shift using signals that pass back and forth between the satellite and ground stations along slant paths, usually track altimeter-bearing satellites. Coincident measurements from at least three such stations are required if the three-dimensional position of the satellite in space, and particularly its altitude, is to be known at the maximum resolution of the tracking system. The distribution of tracking stations is such that a three-dimensional location is seldom possible. The data from an individual tracking system must be used with those data from other stations to construct a global orbit. This provides the required orbit information generalized on a global basis. For this reason, at a particular site and time, the inferred orbit altitude can be in error by a few cm.

Another method employed for precise orbit determination is the use of transponders (Powell, 1986). This allows the altitude of orbit arcs, several thousands of km in length and spanning major oceans, to be located with the same precision so that once every few days the height of the ocean surface under that arc can be measured relative to transponder sites on land with an accuracy of about ± 3 cm. In this method, the predicted orbit of the satellite is used to set the tracking window for the altimeter to view the land-based transponder. When an altimeter passes over a transponder, the latter is illuminated for a few seconds. In this time, a large number of pulses are transmitted and received. The range between the altimeter and the transponder varies in a highly predictable manner and can be expressed as a simple parabolic function of delay time between pulse transmission and reception, and satellite velocity (Powell, 1992). Because the form of the function is known precisely, all the measured pulses can be used to calculate, with very high accuracy, the minimum of that parabola. This minimum corresponds to the delay of pulses transmitted between the altimeter and the transponder at the time of closest approach. The altimeter datastream contains not individual returned pulses but waveforms that are the result of accumulating many returned pulses. The parabola defined by the individual pulses is the same as that defined by the centroid of the waveforms so that the centroid can be used as the measured data. The parabola-fitting process most generally appropriate is an iterative, least-squares-fitting process. The delay measurement is then converted to a range measurement to an estimated accuracy of ± 0.5 cm if the total electron content of the ionosphere, ground-level pressure, and columnar water vapor content of the atmosphere in the region of the transponder are known or if their effects are compensated for.

12.4.2. Correction of Geoid Errors

Several methods have been used for determination of the geoid. One method used accurate tracking of the orbits of various satellites over a long period. Another method relied on measurements of gravity from ships using precision gravimeters. This method provides good spatial details. However, the areas covered by such surveys are limited. In situations in which detailed geoid models are not available, attempts have been made to substitute mean altimetric surfaces. Global mean sea surfaces such as those computed by Marsh and Martin (1982) using this method were not sufficiently accurate for sea-level studies. However, regional surfaces can be generated with a precision appropriate for some applications.

Researchers at NASA's Goddard Space Flight Center have used a portion of the three-month dataset obtained from the Seasat altimeter to derive the topography of the global sea surface with much greater accuracy and detail than has ever been accomplished before. The elevations and depressions have been measured relative to a reference ellipsoid of revolution. The topography resolved small-scale geoidal features due to deep ocean trenches and island arcs (these with signatures of 2−20 meters) as well as the larger geoidal undulations obtained earlier from satellite orbit perturbations and spherical harmonic analyses. This topography includes oceanographic "signals" due to tides and sea-level perturbations arising from a plethora of oceanographically (e.g., currents, gyres) and meteorologically induced causes (e.g., atmospheric pressure loading, wind set-up, and other long-term forces) as well as the geophysical "noise" arising from the gravitational elevations and depressions (i.e., geoidal undulations). The very obvious correlations between the surface topography and the underlying bathymetric features (e.g., deep-sea trenches, island arcs, the continental shelf edge, large seamounts, mid-ocean ridges, and so forth) often seen on the topography map are a manifestation of or contribution from Earth's uncompensated gravitational

elevations and depressions. It is clear, therefore, that much information can be gleaned on the dynamics of the sea surface from the altimetric height measurements if the gravity field of the Earth at close spatial intervals is known precisely. If it were possible to arrive at independent estimates of the marine geoid (say, assembled from marine gravity data) or other means, it could be possible to measure variations in the sea surface elevation with greater precision. The intrinsic accuracies of radar altitude measurements and satellite orbit determination were expected to ultimately allow the goal of obtaining sea surface topography to an accuracy of a few cm. The most severe problem that remained for long was the independent determination of a reference geoid to a precision of a few cm.

12.4.3. Null Methods for Obtaining Topographic Height Variability Independent of Geoid

Detailed knowledge of the marine geoid eluded the oceanographers for a long time, and construction of its model was not an easy task due to lack of knowledge about Earth's gravity field. In the absence of accurate geoid models, two "null" methods have been employed for obtaining the topographic height variability independent of geoid. These are (1) collinear passes and (2) crossover points (i.e., intersections of the satellite ground track with itself).

The most effective of these methods is the collinear-track approach, in which altimeter profiles with nearly identical ground tracks are differenced, tending to eliminate their common geoid signal and revealing time-dependent changes in dynamic height (Brown and Cheney, 1983; Douglas et al., 1987). By subtracting sea surface height from one traverse of the ground track from the height measured on a later traverse, changes in topography can be observed without knowing the geoid. The geoid is constant in time, and the subtraction removes the geoid, revealing changes due to changing currents, such as mesoscale eddies, assuming tides have been removed from the data. It must be noted that altimetric determination of surface ocean circulation is inherently more difficult because of the relatively small signal amplitude as well as the need to separate the dynamic topography from undulations of the geoid as well as from apparent undulations due to radial orbit error. However, for the case of mesoscale eddies, these obstacles have been completely overcome using repeated tracks of altimeter profiles from which geoid and orbit signals can readily be removed. This has resulted in highly accurate maps of sea-height variability attributable to the ocean eddy field. Determination of absolute current velocities will require advances both in geoid modeling and in orbit determination. Some success has been attained, however, using existing geoids and global altimetric surfaces to compute the large-scale surface circulation. Cheney et al. (1983) used the techniques of collinear differences to derive the global mesoscale variability from Seasat altimeter data. The altimeter-measured sea height data appeared to be more reliable than those derived from the XBT-inferred sea heights. However, there are some errors that are not easily removed by the collinear difference method. Increased solar activity causes strong atmospheric density-related altitude measurement fluctuations that are difficult to model.

A technique similar to the collinear tracks uses only the points at which the ascending passes intersect the descending passes (crossovers). Analyses of altimeter crossovers are based on the concept that the geo-potential component of sea level is the same at the intersection of the two tracks at a given point and thus cancels out in the crossover difference. Techniques using crossover differences as input data therefore do not require geoid models. This is of critical importance in the application of altimetry to ocean dynamics because uncertainty of marine geoid models is larger than oceanographic signals of interest (Cheney and Marsh, 1981). When the altimeter-borne satellite orbits in a nonrepeating orbit, it provides a dense network of crossovers. For example, the Geodetic Satellite (Geosat) altimeter provided ~35 million crossovers over the global oceans in a period of 18 months. At each of these locations, the two crossing passes provide independent sea-level measurements at the same place but at different times. Differences of the sea surface heights at the two times, or *crossover differences*, form the basis for variability studies and can also be expressed in terms of sea-level time series.

Generation of time series from altimeter crossover differences involves a separate processing step to convert from height differences (at many combinations of times) to a time-ordered sequence of heights referred to an *arbitrary zero point* (Cheney et al., 1986). The first step is removing radial orbit error. Radial orbit error is eliminated from the reference grid by removing a quadratic trend for each pass in a simultaneous least-squares adjustment. Subsequently, crossover data are grouped into areas that are smaller relative to the horizontal scale of interest (typically a few hundred kilometers). Altimeter data obtained anywhere in the defined area can then be considered representative of the area as a whole. Each crossover difference within the area provides a measure of sea-level change between two discrete times (the times of the two intersecting passes). Once a network of crossover points is generated, the problem confines to the task of solving for a series of individual heights, which are consistent with the height differences. Least-squares techniques are usually used for computing these heights, yielding a time series of sea-level changes at any given grid point from the first altimeter pass to the last.

The task of mapping the Earth's gravity field saw great success in recent years. For example, the joint NASA-German Aerospace Centre Gravity Recovery and Climate Experiment (GRACE) mission—the latest tool for

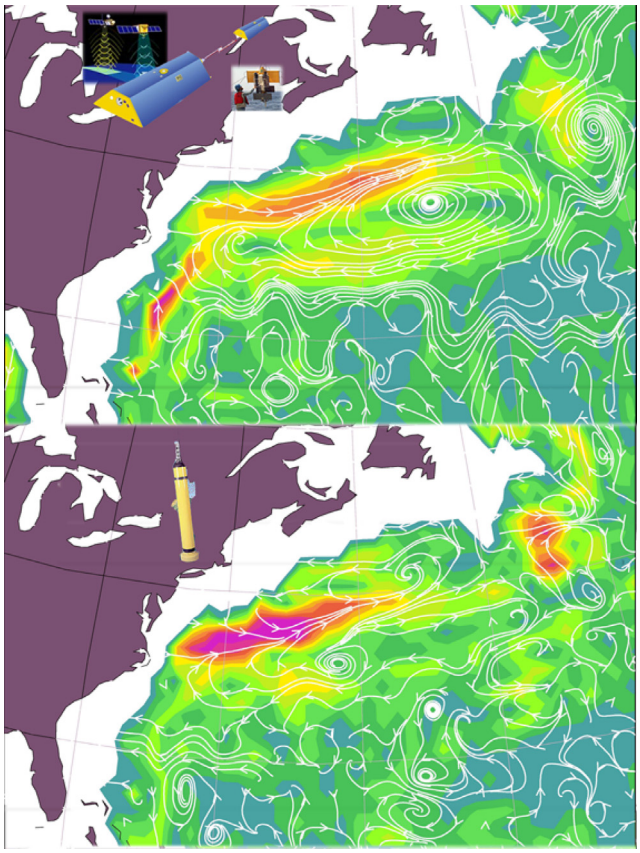

FIGURE 12.7 Ocean currents (depicted by arrows) off the east coast of the United States, 1,000 m beneath the surface. The top panel is obtained from the GRACE geoid, satellite altimetry, and ship measurements of temperature and salt. The bottom panel shows direct measurement of those currents by floats deployed from ships. Colors indicate the strength of the ocean current, with red being strongest and blue-green weakest. Areas in white have no available data. *(Sources: NASA/JPL/University of Texas Center for Space Research/GeoForschungsZentrum (GFZ) Potsdam; http://photojournal.jpl.nasa.gov/catalog/PIA04652; http://photojournal.jpl.nasa.gov/figures/PIA04652-fig3.jpg; Ocean news,* International Ocean Systems*, Sept./Oct. 2003 issue, Vol. 7, Number 5, page 32.)*

scientists working to unlock the secrets of ocean circulation—released its first science product, the most accurate map yet of Earth's gravity field. GRACE senses minute variations in gravitational pull from local changes in Earth's mass by precisely measuring, to a tenth of the width of a human hair, the changes in the separation of two identical spacecrafts following the same orbit approximately 220 km apart. GRACE maps the variations from month to month, following changes imposed by the seasons, weather patterns, and short-term climate change.

The initial gravity model, created from several days of selected GRACE data, represented a major advancement in our knowledge of Earth's gravity field. Pre-GRACE models contained such large errors that many important features were obscured. GRACE brought the true state of the oceans into much sharper focus, so we can now better see ocean phenomena that have a strong impact on atmospheric weather patterns, fisheries, and global climate change. GRACE provided a more precise definition of Earth's geoid, with cm-level precision. Scientists have studied Earth's gravity for decades, using both satellite and ground measurements that were of uneven quality. However, with just a few months' worth of the globally uniform-quality GRACE data, the accuracy of Earth's gravity model has been improved by a factor of between 10 and nearly 100, depending on the size of the gravity feature.

Figure 12.7 shows ocean currents (depicted by arrows) off the east coast of the United States, 1,000 m beneath the surface, obtained from the GRACE geoid, satellite altimetry, and ship measurements of temperature and salt, together with direct measurement of those currents by floats deployed from ships. With advances in gravity field modeling and orbit determination, satellite altimetry is expected to contribute greatly to determination of the general circulation of the oceans (the long-term mean movement of water).

12.5. EVOLUTION OF SATELLITE ALTIMETRY

Radar altimeters carried on spacecraft have provided subtle and valuable data on ocean dynamics by way of measurement of the long and short undulations of the ocean surface. The first such device was part of a payload on Skylab during a short interval in 1972 and was flown as a proof-of-concept instrument (Apel, 1982). The Skylab S-193 altimeter was the first in the series of satellite altimeters that were planned to progressively achieve the goal of detection of global circulation features through sea-level measurements. This altimeter was designed primarily for obtaining the radar measurements necessary for designing improved altimeters. This low-resolution altimeter permitted limited measurements of the sea level. Skylab operated from an altitude of 435 km and used a 100-ns uncompressed pulse of 13.9 GHz for estimation of altitude relative to the sea surface. The Skylab design was that of conventional pulse radar. The beam width of the altimeter radar was 1.5°, providing a footprint of diameter 8 km. The Skylab altimeter could achieve an accuracy of only a few meters. This accuracy was far from satisfactory for estimation of geostrophic currents and detection of mesoscale circulation phenomena such as eddies.

Subsequently, the Geodynamics Experimental Ocean Satellite-3 (GEOS-3 satellite), bearing the second of the series of satellite altimeters, was launched in 1975. This was the first globally applied altimeter system. The GEOS-3 satellite flew at an altitude of 840 km. The altimeter on board this satellite transmitted a chirp frequency of 12.5 ns derived from a 13.9 GHz pulse. The altimeter aboard the GEOS-3 satellite was the first to achieve a precision of approximately 50 cm in height measurement. This was sufficient to measure the 1- to 2-meter sea surface height

difference across the Gulf Stream. In fact, the first altimetric observations of ocean dynamics phenomena took place from the GEOS-3. The GEOS-3 dataset extended over a period of three years and contained a wealth of ocean dynamics information. Using altimeter data from this satellite, Douglas and Gaborski (1979) detected a prominent cold ring, thereby establishing the effectiveness of satellite-borne altimetry in remotely detecting large-scale circulation features. Subsequently, Douglas and Cheney (1981) were able to produce a map of sea surface height variability in the Gulf Stream. Sea surface height variability of other areas such as the Gulf of Mexico and the Caribbean were also mapped in later studies. The GEOS-3 satellite demonstrated the long-term feasibility of such instruments in space for a period in excess of three years.

In an attempt to explore the dynamic ocean features more precisely, NASA launched Seasat in 1978. Seasat was, in fact, the first satellite dedicated to establishing the utility of microwave sensors for remote sensing of the oceans (Born et al., 1979). Seasat circled the earth 14 times a day at an altitude of approximately 800 km. The altimeter directly measured the radial distance (h) from the satellite to the sea surface based on the travel time ($\triangle t$) of very short pulse (3.125 ns chirp waveform) derived from a 13.5 GHz pulse. The Seasat altimeter measurements were supported by a closed-loop microprocessor range tracker and an automatic gain-control feedback loop. Because the spacecraft's longitudinal axis was oriented toward the geocenter to $\pm 0.5^{\circ}$, the measured distance was very nearly in the direction defined by the geodetic vertical at the subsatellite point (Schutz et al., 1982). Microwave pulses were transmitted at a repetition rate of 1,020 Hz. The altitude information thus obtained was compressed and recorded on board the spacecraft to yield 10 data points per second. Further ground-based processing applied necessary smoothing to produce altimetric measurements at the rate of one per second. From an altitude near 800 km, it measured the satellite-to-surface separation with a precision better than 10 cm, for an overall distance accuracy of better than 12 parts per million.

The radar altimeter flown on Seasat collected approximately 1,000 orbits of continuous data around the world before it failed in orbit because of a reported short circuit in the electrical power system. However, the data collected by the Seasat altimeter represented about 90 percent of the data collected by the GEOS-3 radar altimeter during its 3.5 years of operation (Townsend, 1980). The Seasat altimeter data, together with a detailed gravimetric geoid, have been used to demonstrate the ability of satellite altimetry to detect sea surface height signatures associated with the Gulf Stream system. The presence of dynamic ocean features in the altimeter profiles was verified by comparison with standard oceanographic observations gathered from a variety of sources during the Seasat mission (Cheney, 1982).

The Seasat altimeter was a remarkable instrument that yielded information on sea surface topography and demonstrated the enormous potential of altimetry for oceanographic studies. The relatively short duration of the Seasat altimetric mission could not realize the full potential of the altimeter's "all-weather" observations of ocean fronts and eddies. A follow-on altimeter mission was expected to yield obvious benefits. Accordingly, Geosat, funded by the U.S. Navy, was launched in 1985. This was the first satellite altimeter to provide long-term global coverage. The primary purpose of this satellite was improvement of our knowledge of the marine gravity field. Geosat carried a 13.5-GHz radar altimeter that provided a continuous record of sea level along the satellite ground track. Geosat was, in fact, an improved version of the Seasat altimeter. A ground station provided information on the satellite ephermeris as well as tidal and other corrections. In April 1985, Geosat began generating a remarkable dataset that changed the way in which physical oceanographers viewed the global oceans.

During the initial 18 months of "primary mission" operation, data from Geosat was downloaded to Johns Hopkins University's Applied Physics Laboratory (APL) every 12 hours. At APL, the altimeter data were processed, enabling determination of sea-level variability and providing applications in many areas of ocean dynamics. One of the initial applications was to yield information on the ice edge on a global basis as well as oceanic fronts and eddies only from the northwest Atlantic regions encompassing the Gulf Stream. In September 1986, at the conclusion of the initial mission, Geosat was placed into a near-Seasat 17-day repeat orbit. The altimeter data collected during this Exact Repeat Mission (ERM) has been used to determine locations of ocean fronts and eddies over more of the ocean's surface than during the initial 18 months of operation. The information gathered from Geosat was routinely used in support of a variety of oceanographic parameters as well as fleet operations of naval interest (Cummings, 1988).

Although neither the Geosat nor the Seasat records were sufficient for definitive analyses of a global nature, Geosat established a new milestone in satellite oceanography by the duration and coverage of its observations. It is the first altimeter satellite to make continuous, global, multiyear measurements. During the first 18 months, Geosat accumulated 270 million sea-level observations along 200 million km of the world oceans, with a precision approaching 2 cm (Cheney et al., 1986). In a field historically limited by lack of observations, the Geosat datasets were the most extensive oceanographic datasets ever collected. These datasets offered a preview of future altimeter missions and provided a unique opportunity to gain experience in the analysis of global ocean datasets.

Altimeter technology has rapidly evolved since the first radar altimeter was flown on Skylab in 1973. Several satellite altimeter systems have been launched that have the capability

to measure the range of radar altimeter signals returned from the sea surface with a variance of about ±3 cm for sea state of about $H_s = 2$m and only slightly worse for much higher sea states. The utility of satellite altimetry for measuring ocean currents and circulation features through measurement of sea-level elevation variability has been demonstrated by a series of altimeters of increasing accuracy and precision, flown successively on several subsequent satellites.

The role of satellite altimetry in the study of global ocean circulation has been remarkable. The GEOS-3, Seasat, and Geosat experiments demonstrated that satellite altimeter technology can provide the mechanism for monitoring the oceans on a scale that appropriates the requirements of oceanographers. With the launch of the ERS-1 satellite, altimetry data began to be collected on a global scale. The first systems, carried on Seasat, Geosat, ERS-1, and ERS-2, were designed to measure week-to-week variability of currents. Topex/Poseidon, launched in 1992, was the first satellite designed to make the much more accurate measurements necessary for observing the permanent (time-averaged) surface circulation of the oceans, tides, and variability of gyre-scale currents. This was replaced by Jason in 2001. Topex/Poseidon and Jason flew over the same ground track every 9.9156 days. The great accuracy and precision of the Topex/Poseidon and Jason altimeter systems allowed them to measure the oceanic topography over ocean basins with an accuracy of ±5 cm. This allowed them to measure:

- Changes in the mean volume of the ocean
- Seasonal heating and cooling of the ocean
- Tides
- The permanent surface geostrophic current system
- Changes in surface geostrophic currents on all scales
- Variations in the topography of equatorial current systems such as those associated with El Niño

Plotting the global distribution of time-averaged topography of the ocean surface provides a means of obtaining the global distribution of geostrophic currents at the ocean surface. The authenticity of altimetric detection of mesoscale dynamic events had been proved based on comparison with measurements obtained from satellite-tracked drifters circling the eddies during the same time when altimetric data were collected from the same location (Cheney and Marsh, 1981). Similarly, the Gulf Stream path depicted by the Seasat altimeter data closely agreed with the satellite infrared imagery during the time. These intercomparison experiments provided a high degree of confidence in the altimetric technique of remote sensing of ocean circulation features. It must, however, be accepted that although satellite altimetry has several merits, the technique does not have the capability to detect and quantify the entire range of surface circulation features. The technique is applicable to measurements of ocean circulation features of only large space scales.

Aviso has been distributing altimetric data worldwide since 1992. Consideration is now being given to altimetry missions capable of "scanning" the ocean surface to acquire data at scales of a few tens of kilometers, passing over the same spots every few days. The goal will be to monitor relatively rapid ocean variations over a period of less than 10 days at scales below 100 km. On February 28, 2013, the Indian Space Research Organization (ISRO) satellite successfully launched a CNES (France)-built Saral (Satellite with ARgos and ALtika). The altimeter (working in Ka-band, 35 GHz), named ALtika, will enable better observation of coastal zones. Land-based sea-level gauges will be used for calibration of the altimeter. In the Indian Ocean region, a network of four microwave radar gauges, which form part of a larger network, the Integrated Coastal Observation Network (ICON), for real-time monitoring of sea-level, sea-state, and surface meteorological data (Prabhudesai et al., 2010) developed by CSIR-National Institute of Oceanography, India has already been installed for this purpose.

REFERENCES

Apel, J.R., 1982. Some recent scientific results from the Seasat altimeter. Sea Technol. 23 (10), 21–27.

Barrick, D.E., Swift, C.T., 1980. The Seasat microwave instruments in historical perspective. IEEE J. Oceanic Eng. OE-5 (2), 75–79.

Biggs, A.W., Jordan, J.M., 1989. Simulation of chirp pulse spectra and effect of Doppler shifts on backscattered pulses. Quantitative Remote Sensing: An Economic Tool for the Nineties 3, 1720–1722.

Bonjean, F., Lagerloef, G.S.E., 2002. Diagnostic model and analysis of the surface currents in the tropical Pacific Ocean. J. Phys. Oceanogr. 32 (10), 2938–2954.

Born, G.H., Dunne, J.A., Lame, D.B., 1979. Seasat mission overview. Science 204, 1405–1406.

Brown, O.B., Cheney, R.E., 1983. Advances in satellite oceanography: Reviews of geophysics and space physics 21 (5), 1216–1230.

Cheney, R.E., 1982. Comparison data for Seasat altimetry in the Western North Atlantic. J. Geophys. Res. 87 (C5), 3247–3253.

Cheney, R.E., Marsh, J.G., 1981. Oceanographic evaluation of geoid surfaces in the Western North Atlantic. In: Gower, J. (Ed.), Oceanography from space. Plenum, New York, NY, USA, pp. 855–864.

Cheney, R.E., Marsh, J.G., 1981. Seasat altimeter observations of dynamic topography in the Gulf Stream region. J. Geophys. Res. 86 (C1), 473–483.

Cheney, R.E., Douglas, B.C., Sandwell, D.T., Marsh, J.G., Martin, T.V., McCarthy, J.J., 1984. Applications of satellite altimetry to oceanography and geophysics. Mar. Geophys. Res. 7, 17–32.

Cheney, R.E., Douglas, B., Agreen, R., Miller, L., Milbert, D., Porter, D., 1986. The Geosat altimeter mission: A milestone in satellite oceanography. Eos 67 (48), 1354–1355.

Cheney, R.E., Marsh, J.G., Beckley, B.D., 1983. Global mesoscale variability from repeat tracks of Seasat Altimeter data. J. Geophys. Res. 88, 4342–4354.

Cheney, R.E., Emery, W.J., Haines, B.J., Wentz, F., 1991. Recent improvements in Geosat altimeter data. Eos 72 (51), 577–580.

Clay, C.S., Medwin, H., 1977. Acoustical oceanography: Principles and applications. Wiley-lnterscience, Newyork.

Cummings, T.K., 1988. Geosat: Navy applications of satellite altimetry growing. Sea Technol. 29 (11), 39–43.

Douglas, B.C., Gaborski, P.D., 1979. Observation of sea surface topography with GEOS-3 altimeter data. J. Geophys. Res. 84 (B8), 3893–3896.

Douglas, B.C., Cheney, R.E., 1981. Ocean mesoscale variability from repeat tracks of GEOS-3 altimeter data. J. Geophys. Res. 86 (C11), 10,931–10,937.

Douglas, B.C., McAdoo, D.C., Cheney, R.E., 1987. Oceanographic and geophysical applications of satellite altimetry. Rev. Geophys. 25 (5), 875–880.

Fu, L.L., Chelton, D., 2001. Large-scale ocean circulation. In: Fu, L.L., Cazenave, A. (Eds.), Satellite altimetry and earth sciences: A handbook of techniques and applications. Academic Press, pp. 133–169.

Fu, L.L., Chelton, D.B., Zlotnicki, V., 1988. Satellite altimetry: Observing ocean variability from space. Oceanography (Feature).

Hurlburt, H.E., Hogan, P.J., 2008. The Gulf Stream pathway and the impacts of the eddy-driven abyssal circulation and the Deep Western Boundary Current. Dynamics of Atmospheres and Oceans 45, 71–101.

Joseph, A., 2000. Applications of Doppler Effect in navigation and oceanography. In: Encyclopedia of Microcomputers, vol. 25. Marcel Dekker, New York, NY, USA. pp. 17–45.

Levitus, S., 1982. Climatological atlas of the world ocean. NOAA Professional Paper 13, Rockville, MD, 20852, USA.

Lorell, J., Colquitt, E., Anderle, R.J., 1982. Ionospheric correction for Seasat altimeter height measurement. J. Geophys. Res. 87 (C5), 3207–3212.

MacArthur, J.L., 1976. Design of the Seasat-A radar altimeter. Proc. Oceans '76 IEEE Conference, 10B-1–10B-8.

Marsh, J.G., Martin, T.V., 1982. The Seasat altimeter mean sea surface model. J. Geophys. Res. 87 (C5), 3269–3280.

Neumann, G., 1968. Ocean currents. Elsevier, Amsterdam- London- New York.

Powell, R.J., 1986. Relative vertical positioning using ground-level transponders with the ERS-1 altimeter. IEEE Trans. Geosci. Remote Sensing GE-24 (3), 421–425.

Powell, R.J., 1992. Measurement of mid-ocean surface levels to ±3 cm with respect to mid-continent reference points using transponders with the ERS-1 and Topex altimeters: A developing technique. Workshop Report No. 81, Intergovernmental Oceanographic Commission, 111–119.

Prabhudesai, R.G., Joseph, A., Agarwadekar, Y., Mehra, P., Vijay Kumar, K., Luis, R., 2010. Integrated Coastal Observation Network (ICON) for real-time monitoring of sea-level, sea-state, and surface meteorological data. Oceans '10: IEEE Seattle Technical Conference. September 2010.

Raney, R.K., 1998. The Delay/Doppler radar altimeter. IEEE Trans. Geosci. Remote Sensing 36 (5), 1578–1588.

Robinson, I.S., 1985. Satellite Oceanography, An introduction for oceanographers and remote sensing scientists. Ellis Horwood Ltd, Chichester.

Schutz, B.E., Tapley, B.D., Shum, C., 1982. Evaluation of the Seasat altimeter time tag bias. J. Geophys. Res. 87 (C5), 3239–3245.

Sverdrup, H.U., Johnson, M.W., Fleming, R.H., 1942. The oceans: Their physics, chemistry, and general biology. Prentice Hall, New York, NY, USA.

Tapley, B.D., Born, G.H., Parke, M.E., 1982. The Seasat altimeter data and its accuracy assessment. J. Geophys. Res. 87 (C5), 3179–3188.

Townsend, W.F., 1980. An initial assessment of the performance achieved by the Seasat-1 radar altimeter. IEEE J. Oceanic Eng. OE-5 (2), 80–92.

Ulaby, F.T., Moore, R.K., Fung, A.K., 1982. Microwave remote sensing (active and passive). In: Radar Remote Sensing and Surface Scattering and Emission Theory, vol. II. Addison-Wesley Advanced Book Program/World Science Division, Reading, Massachusetts, 1064.

Wunsch, C., 1986. Calibrating an altimeter: How many tide gauges is enough? J. Atmos. Oceanic Technol. 3, 746–754.

Wunsch, C., Gaposchkin, E.M., 1980. On using satellite altimetry to determine the general circulation of the ocean with application to geoid improvement. Rev. Geophys. 18, 725–745.

Wyrtki, K., 1977. Sea level during the 1972 El Niño. J. Phys. Oceanogr. 7 (6), 779–787.

BIBLIOGRAPHY

Bernstein, R.L., Born, G.H., Whritner, R.H., 1982. Seasat altimeter determination of ocean current variability. J. Geophys. Res. 87 (C5), 3261–3268.

Cheney, B., Miller, L., Agreen, R., Doyle, N., Lillibridge, J., 1994. Topex/Poseidon: The 2-cm solution. J. Geophys. Res. 99, 24,555–24,564.

Cheney, R.E., Marsh, J.G., 1982. Ocean currant detection by satellite altimetry. Proc. Oceans '82 Conference, 409–414.

Cheney, R.E., Douglas, B.C., Miller, L., 1989. Evaluation of Geosat altimeter data with application to tropical Pacific sea-level variability. J. Geophys. Res. 94, 4737–4748.

Cheney, R.E., Marsh, J.G., Beckley, B.D., 1983. Global mesoscale variability from collinear tracks of Seasat altimeter data. J. Geophys. Res. 88 (C7), 4343–4354.

Cheney, R.E., Emery, W.J., Haines, B.J., Wentz, F., 1991. Recent improvements in Geosat altimeter data. Eos 72 (51), 577–580.

Cutting, E., Born, G.H., Frautnik, J.C., 1978. Orbit analysis for Seasat-A. J. Astronaut. Sci. XXVI, 315–342.

Delcroix, T., Boulanger, J.P., Masia, F., Menkes, C., 1994. Geosat-derived sea level and surface current anomalies in the equatorial Pacific during the 1986–1989 El Niño and La Niña. J. Geophys. Res. 99, 25,093–25,107.

Diamante, J.M., Douglas, B.C., Porter, D.L., Masterson, R.P., 1982. Tidal and geodetic observations for the Seasat altimeter calibration experiment. J. Geophys. Res. 87 (C5), 3199–3206.

Diamante, J.M., Pyle, T.E., Carter, W.E., Scherer, W.D., 1987. Global change and the measurement of absolute sea level, Progress in Oceanography. Pergamon Press.

Douglas, B.C., Cheney, R.E., 1990. Geosat: Beginning a new era in satellite oceanography. J. Geophys. Res. 95 (C3), 2833–2835.

Douglas, B.C., McAdoo, D.C., Cheney, R.E., 1987. Oceanographic and geophysical applications of satellite altimetry. Rev. Geophys. 25 (5), 875–880.

Kao, T.W., Cheney, R.E., 1982. The Gulf Stream front: A comparison between Seasat altimeter observations and theory. J. Geophys. Res. 87 (C1), 539–545.

Kolenkiewicz, R., Martin, C.F., 1982. Seasat altimeter height calibration. J. Geophys. Res. 87 (C5), 3189–3197.

Legeckis, R., 1987. Satellite observations of a western boundary current in the Bay of Bengal. J. Geophys. Res. 92 (C1 2), 12,974–12,978.

McGoogan, J.T., Miller, L.S., Brown, G.S., Hayne, G.S., 1974. The S193 radar altimeter experiment. Proc. IEEE 62 (6), 793–803.

Miller, L., Cheney, R.E., 1990. Large-scale meridional transport in the tropical Pacific Ocean during the 1986-87 El Niño. J. Geophys. Res. 95 (17), 905–920.

Miller, L., Cheney, R.E., Douglas, B.C., 1988. Geosat altimeter observations of Kelvin waves and the 1986–87 El Niño. Science 239, 52–54.

Mitchum, G.T., 1994. Comparison of Topex sea surface heights and tide gauge sea levels. J. Geophys. Res. 99 (C12), 24,541–24,553.

Parker, B.B., Cheney, R.E., Carter, W.E., 1992. NOAA global sea-level program. Sea Technol. 33 (6), 55–62.

Ponte, R.M., Lyard, F., 2002. Effects of unresolved high-frequency signals in altimeter records inferred from tide gauge data. J. Atmos. Oceanic Technol. 19 (4), 534–539.

Rossby, H.T., 1983. Eddies and the general circulation. In: Brewer, P.G. (Ed.), Oceanography; The present and future. Springer-Verlag, New York, Heidelberg, Berlin, pp. 137–161.

Schwiderski, E.W., 1991. High-precision modeling of mean sea level, ocean tides, and dynamic ocean variations with Geosat altimeter signals. In: Parker, B.B. (Ed.), Tidal Hydrodynamics. Wiley, New York, NY, USA, pp. 593–616.

Tai, C.K., White, W.B., Pazan, S.E., 1989. Geosat crossover analysis in the tropical Pacific, 2. Verification analysis of altimetric sea-level maps with expendable bathythermograph and island sea level data. J. Geophys. Res., 94,897–94,908.

Tapley, B.D., Born, G.H., Hager, H.H., Lorell, J., Parke, M.E., Diamante, J.M., Douglas, B.C., Goad, C.C., Kolenkiewicz, R., Marsh, J.G., Martin, C.F., Smith III, S.L., Townsend, W.F., Whitehead, J.A., Byrne, H.M., Fedor, L.S., Hammond, D.C., Mognard, N.M., 1979. Seasat altimeter calibration: Initial results. Science 204 (4400), 1410–1412.